Iranian Journal of Science & Technology, Transaction B, Engineering, Vol. 33, No. B5, pp 441-452
Printed in The Islamic Republic of Iran, 2009

NUMERICAL SIMULATION OF THE MOTION OF A SINGLE DROP IN A SHEAR FLOW AT FINITE REYNOLDS NUMBERS*

M. BAYAREH AND S. MORTAZAVI**

Dept. of Mechanical Engineering, Isfahan University of Technology (IUT), I. R. of Iran
Email: saeedm@cc.iut.ac.ir

Abstract– Three-dimensional numerical simulation of the cross-stream migration of a drop in simple shear flow at finite Reynolds numbers neglecting the gravity influence is presented. In this study the full Navier-Stokes equations are solved by a finite difference/front tracking method. A drop is shown to migrate to the centreline of the channel in a shear flow. In other words, the centre of the channel is a global attractor of trajectories of a drop, regardless of the initial position and velocity. The migration velocity of the drop depends on surface tension and fluid velocity. Increasing the Weber number and decreasing the Reynolds number decrease the time of the migration to the centreline. The study showed that after an initial transient period the drop leads the local undisturbed velocity, for all cases. While time progresses, the velocity of the drop along the flow direction (x) decreases, whereas the velocity of drop along the flow velocity gradient increases. When the x-velocity reaches the local undisturbed velocity, the slip velocity tends to zero, except during a short initial transient. The slip velocity is the difference between the drop velocity and the ambient fluid velocity at the centre of the drop for the undisturbed flow. To validate the present calculations, some typical results are compared with the available experimental and theoretical data, which confirm that the present approach is qualitatively reliable in predicting the drop migration.

Keywords– Drop migration, shear flow, front-tracking method, finite difference method, Reynolds number, Weber number

1. INTRODUCTION

Many flows contain buoyant particles that are rigid or deformable. Polymer flows, fuel sprays and the motion of red blood cells are some such examples. In polymer processing, the concentration of particles across the channel is of great interest. The cross-stream migration of particles in a shear flow affects the local concentration of particles across the channel. The problem of particle motion in shear flows has always been of great interest. Experimentally, the phenomena have been measured (initially by Taylor) [1] even though the shear flows considered have been restricted in most investigations to simple shear in a Couette device. Karnis *et al.* [2] reported that neutrally buoyant particles stabilized midway between the centreline and the wall in a channel, closer to the wall for larger flow rates and closer to the centre for larger particles. Halow and Wills [3] did experiments in a concentric cylindrical Couette device. They observed that when the inner cylinder rotates, a particle migrates from any initial position to equilibrium at a small distance inside the centreline of the gap. Rallison [4] studied the time-dependent deformation and burst of a viscous drop in an arbitrary shear flow at zero Reynolds number. He presented a numerical scheme to track the two-dimensional drop shape in time. Mola *et al.* [5] introduced a simple model for prediction of pressure drop in horizontal two-phase flows. Magna and Stone [6] reported the time-dependent interactions between two buoyancy-driven deformable drops in a low Reynolds number flow.

*Received by the editors August 30, 2008; Accepted July 11, 2009.
**Corresponding author

They introduced three modes for film drainage between the drops: rapid drainage, uniform drainage and dimple formation. As the separation distance between the two drops decreases, the mode of film drainage may change from rapid drainage to uniform drainage and eventually a dimple may form. Zhou and Pozrikidis [7] studied the flow of periodic suspension of two-dimensional viscous drops in a closed channel bounded by two parallel plane walls. They found that a critical capillary number exists, below which the suspensions exhibit stable periodic motion, and above which the drops elongate and tend to coalesce, altering the topology of the initial configuration. The effects of capillary number, viscosity ratio, volume fraction of dispersed phase, lattice geometry, and instantaneous drop shape on the effective stress tensor of the suspension were also studied. Feng *et al.* [8] reported the results of a two-dimensional finite element simulation of the motion of a circular particle in a Couette and Poiseuille flow. They showed that a neutrally buoyant particle migrates to the centerline in a Couette flow and the stagnation pressure on the particle surface is particularly important in determining the direction of migration. Li, Zhou and Pozrikidis [9] studied the motion of two-dimensional, doubly periodic, dilute and concentrated emulsions of liquid drops with constant surface tension in a simple shear flow. Their numerical method is based on a boundary integral formulation. They showed that the shearing flow is able to stabilize a concentrated emulsion against the tendency of the drops to become circular and coalesce, thereby allowing for periodic evolution even when the volume fraction of the suspended phase might play a role similar to that of the foam. Loewenberg and Hinch [10] did a three-dimensional simulation of a concentrated emulsion in shear flow for zero-Reynolds-number and finite-capillary-numbers. Results were obtained for dispersed-phase volume fractions up to 30% and dispersed to continuous-phase viscosity ratios in the range of 0 to 5. They reported the viscosity of an emulsion is only a moderately increasing function of the dispersed-phase volume fraction, in contrast to suspensions of rigid particles or undeformed drops. Esmaeeli and Tryggvason [11] simulated the motion of two-and three-dimensional buoyant bubbles. They compared a finite Reynolds number two-dimensional simulation with sixteen bubbles and a Stokes flow simulation and reported that the finite Reynolds number array break up much faster. Their simulations showed a slight increase in the average rise velocity compared to a regular array. Mortazavi and Tryggvasson [12] studied the motion of a drop in Poiseuille flow. They simulated the motion of many drops at finite Reynolds numbers. Esmaeeli and Tryggvason [13] simulated the motion of two-and three-dimensional finite Reynolds number buoyant bubbles. It was shown that the rise in the Reynolds number is nearly independent of the number of bubbles, as the velocity fluctuations in the liquid (the Reynolds stresses) increase with the size of the system. Balabel *et al.* [14] introduced a numerical model based on the level set method for computing unsteady droplet internal flows and presented this model for linear droplet oscillation processes. Crowdy [15] studied the problem of a two-dimensional inviscid compressible bubble evolving in Stokes flow. They reported that if the ambient pressure is small enough, bubbles can expand significantly. In addition, they showed that a bubble evolving adiabatically is less likely to expand than an isothermal bubble. Yoon *et al.* [16] investigated, experimentally, the effect of the dispersed to continuous-phase viscosity ratio on the flow-induced coalescence of two equal-sized drops with clean interfaces. Their study showed that when the viscosity ratio is greater than O(0.1), the critical capillary number decreases with increasing the offset only for the smallest offsets, but increases with increasing the offset until a critical offset is reached above which coalescence is not observed. Norman *et al.* [17] studied the neutrally buoyant particles in a low-Reynolds-number pressure-driven flow. They showed that when the particle density differs from that of the suspending fluid, buoyancy forces also affect particle migration. They reported that suspension flows become fully developed earlier than that observed for neutrally buoyant particles. Yang *et al.* [18] simulated the migration of a sphere in tube flow. They presented a formula for the lift force. Their formula predicted the change in the sign of the lift force. Their correlation formula was compared with analytical lift formula and showed that the equilibrium position moves toward

the wall as the Reynolds number increases at a fixed drop radius, and it moves towards the centreline as the radius of the drop increases at a fixed Reynolds number.

Sibillo *et al*. [19] investigated the deformation and breakup of a drop in an immiscible equiviscous liquid undergoing unbounded shear flow. They showed that wall effects can be exploited to obtain nearly monodisperse emulsions in microconfined shear flow. Zhao [20] investigated the drop break up in dilute Newtonian emulsions in simple shear flow by using high-speed microscopy over a wide range of viscosity ratios, focusing on a high capillary number. He showed that the final drop size distribution intimately links to the drop break up mechanism, which depends on the viscosity ratio and the capillary number.

Theoretical analysis of the lateral migration of deformable drops in a channel flow was restricted to the two-dimensional Stokes and potential flows. In this paper we study the migration of a drop in simple shear flow at finite Reynolds numbers by adding the advection terms to the governing equations.

Section 2 contains the formulation, introduction of the governing non-dimensional parameters, and a short description of the numerical method.

2. FORMULATION AND NUMERICAL METHOD

a) Formulation

The governing equations for the motion of unsteady, viscous, incompressible, immiscible two- fluid systems are the Navier-Stokes equations in conservative form:

$$\frac{\partial \rho u}{\partial t} + \nabla .\rho uu = -\nabla P + \nabla .\mu(\nabla u + \nabla u^T) + \sigma \int \kappa n \delta^{\beta}(x - X) d_S \tag{1}$$

Here u is the fluid velocity, p is the pressure, ρ is the fluid density, μ is the fluid viscosity, and σ is the surface tension coefficient. Also, δ^{β} is a two- or three-dimensional delta function, respectively, for $\beta = 2$, and $\beta = 3$. κ is the curvature for two-dimensional flows and twice the mean curvature for three-dimensional flows. n is a unit vector normal to the drop surface pointing outside of the drop. x is the position in a Eulerian coordinate and X is the position of the front in Lagrangian coordinate.

Both immiscible fluids are taken to be incompressible, so the divergence of the velocity field is zero:

$$\nabla .u = 0 \tag{2}$$

Equations of state for the density and the viscosity are:

$$\frac{D\rho}{Dt} = 0 \quad , \quad \frac{D\mu}{Dt} = 0 \tag{3}$$

These equations show that the density and the viscosity of each fluid remain constant.

Unlike the velocity that is taken to be continuous, the pressure jumps across the interface. Continuity of stresses at the fluid boundary shows that the normal stresses are balanced by surface tension. The force due to surface tension is

$$\Delta F = \sigma kn \tag{4}$$

The two governing non-dimensional numbers of the flow are the Reynolds number and the Weber number. The Reynolds number is defined in different ways: A bulk Reynolds number is defined based on the shear rate and channel height. A particle Reynolds number is defined based on the shear rate and drop radius:

$$\mathrm{Re}_b = \frac{\rho_0 G H^2}{\mu_0} \quad , \qquad \mathrm{Re}_P = \frac{\rho_0 G a^2}{\mu_0} \quad , \qquad We = \frac{\rho_0 G^2 a^3}{\sigma} \tag{5}$$

Here ρ_0 is the density of ambient fluid, μ_0 is the viscosity of the ambient fluid, a is the initial radius of the drop, H is the height of the channel and G is the shear rate. Shear rate is

$$G = \frac{u_t - u_b}{H} \tag{6}$$

where u_t and u_b are the velocity of top and bottom walls, respectively.

In this work, the ratios of the drop density and viscosity to that of the ambient fluid are considered as one.

b) Numerical method

Various methods have been used to simulate the two-phase flows. These methods include the marker-and-cell (MAC) method, the volume-of-fluid (VOF) method, and the level set method. In general, the interface representation can be explicit (moving mesh) or implicit (fixed mesh) or a combination of both. The front-tracking method is a combination of the fixed and moving mesh method. Although an interface grid tracks the interface, the flow is solved on a fixed grid. The interface conditions are satisfied by smoothing the interface discontinuities and interpolating interface forces from the interface grid to the fixed grid. In this method, the governing equations are solved for the whole flow field. Front capturing has two difficulties. The first is a sharp boundary between the fluids, and the second is accurate computation of surface tension. Different attempts have been made in overcoming these problems.

For the simulations presented here, the method developed by Unverdi and Tryggvason [21] is used. They simulated the motion of buoyant bubbles in a periodic domain. Equations (2-1), (2-2), and (2-3) are solved in a rectangular three-dimensional domain with a finite difference method. The spatial differentiation is calculated by second order finite difference on a staggered Eulerian grid. We use an explicit second-order time integration method. Combining the incompressibility condition and momentum equations results in a non-separable elliptic equation for the pressure. Due to the similarity in density between the drop and the ambient fluid, a fast Poisson solver (FISHPACK) solves the pressure equation.

In the three-dimensional flow, the average surface curvature is

$$\kappa n = (n \times \nabla) \times n \tag{7}$$

Then, the force on each element surface is

$$\delta F_\sigma = \sigma \int_{\sigma A} \kappa n d_A = \sigma \int_{\sigma A} (n \times \nabla) \times n d_A = \sigma \oint_S t \times n d_S \tag{8}$$

The integration is over the boundary of each element representing the front. t and n are the tangent and the normal vector to each element, respectively.

3. RESULTS

We now consider the cross-stream migration of a drop in a simple shear flow. The diameter of the drop is a, and the height of the channel is $H = 10/3\ a$ so that $\xi = a/H = 0.3$. ξ is the geometric ratio. The top wall in z-direction is moving at velocity U and the bottom wall is stationary. The boundary conditions are periodic in the x- and y-direction and rigid, top and bottom walls in the z-direction (Fig. 1).

Perturbation theories of viscous or inertial type are valid for small particle Reynolds numbers, i.e. $Re_p << \xi^2$ (Ho and Leal [22]). This condition is not satisfied in our study. For the calculations in this paper, we use Re_b as equal to 5, 10, and 15. So that Re_p becomes 0.1125, 0.225, and 0.3375, respectively, and these values are greater than $\xi^2 = 0.09$.

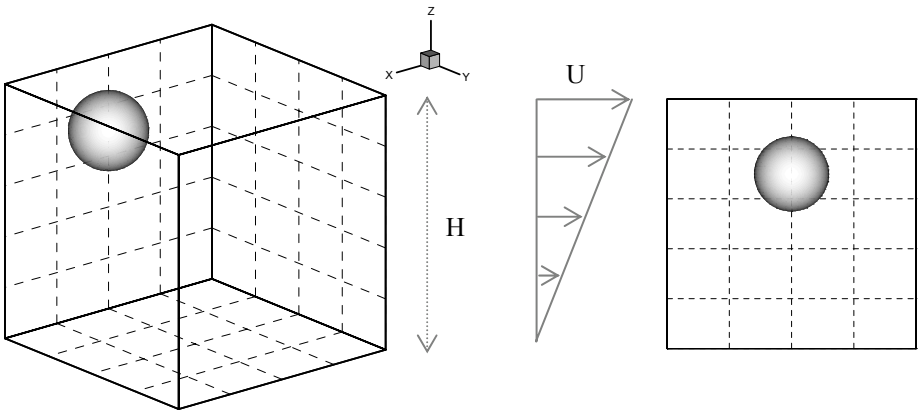

Fig. 1. Migration of a drop in a simple shear flow between no-slip walls

Since the computational resources are directly proportional to the size of the stationary grid, we must find a compromise between the numbers of grid points required to resolve a drop. Figure 2 shows the migration of a three-dimensional drop at Re_b = 10 and We = 0.0675 that is computed on 66×34×66, 48×26×48, and 34×18×34 grids. Time is normalized by the shear rate G. Resolution test yields almost similar results. Since run time depends directly on the size of the grid, we have selected the coarse grid for our simulations.

Figure 3 shows the streamlines in the middle section in y-direction at Re_b = 10 and We = 0.0675, computed on a 34×18×34 grid. The drop diameter is 0.3 times the size of the periodic domain, and therefore we have about 10 grid points per drop diameter in the x- and z-direction. The streamlines sketched are based on the difference between the velocity of each point and the velocity of the drop centre. This figure shows a rotation of drop that is one of the factors responsible for the drop migration. The basic mechanism of the migration is discussed later.

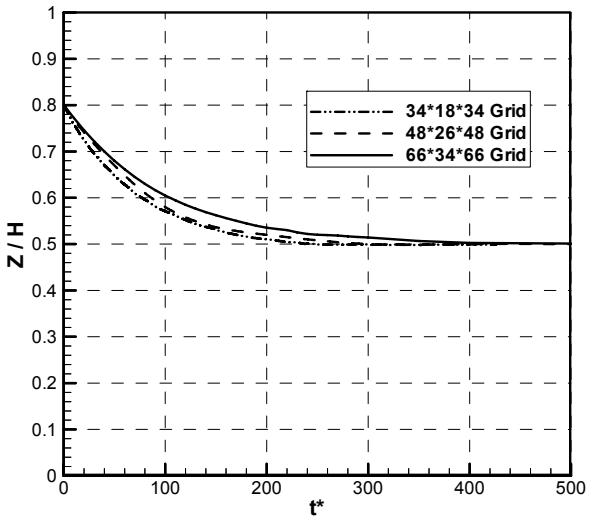

Fig. 2. Lateral migration of a drop in a simple shear flow at Re_b = 10 and We = 0.0675

Figure 4 shows the lateral migration of drops in a simple shear flow at different initial positions. The numerical results which can be compared to our simulations are the ones by Feng *et al*., who simulated the migration of a rigid particle at Re_b = 40 in a simple shear flow and obtained similar results. It is seen that the drop always migrates to the centre of the channel, regardless of the initial position. In other words, the

centre of the channel is a global attractor of the trajectories of a drop. The perturbation solutions also predict that the centre is a stable equilibrium position (Feng *et al.*). The effects of the surface tension and the velocity are discussed later.

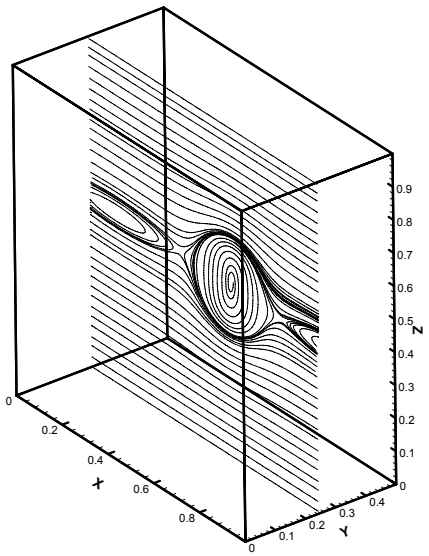

Fig. 3. The shape of the streamlines in the middle section in y-direction at $Re_b = 10$ and $We = 0.0675$, computed on a $34 \times 18 \times 34$ grid

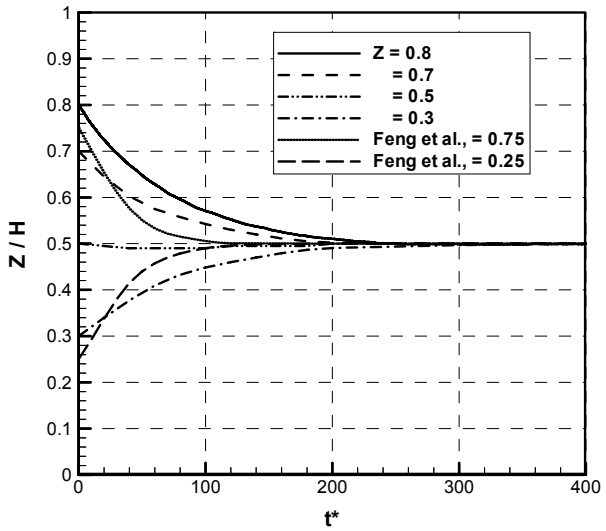

Fig. 4. Comparison of the Lateral migration of a drop in a simple shear flow predicted by our simulations and the numerical results of Feng *et al*. (1994). In our simulation, $Re_b = 10$ and $We = 0.0675$. In the simulations of Feng *et al*., $Re_b = 40$, $\xi = 0.125$

Experimental results which can be compared to our simulations are the results obtained by Halow and Willis. Because of the difference in geometry, we are unable to construct a characteristic time to compare the speed of migration in both studies. So we have plotted the drop trajectories in Fig. 5 versus t^* / Re_p predicted in our simulation compared to those observed by Halow and Willis in a cylindrical Couette device.

To investigate the drop shape evolution, a scalar measure of the drop deformation (the Taylor deformation) by $D = (l\text{-}b)/(l+b)$ is calculated, where l, b are the major and minor semi-axes of the drop

(defined by the largest and smallest distances of the surface from the centre of the drop). The deformation of a drop is an increasing function of the Weber number. In other words, the deformation decreases with the increasing magnitude of the surface tension. Figure 6 shows the shape of a drop in a simple shear flow at a fixed Reynolds number Re_b = 10, which includes: initial time (6-a), We = 0.09 (6-b) and We = 0.27 (6-c). In Figs. 6-b, and c, the non-dimensional time is t^* = 9. In Fig. 7, we have plotted the deformation (D) versus dimensionless time. It can be seen that the deformation increases with increasing time and rapidly reaches the steady value.

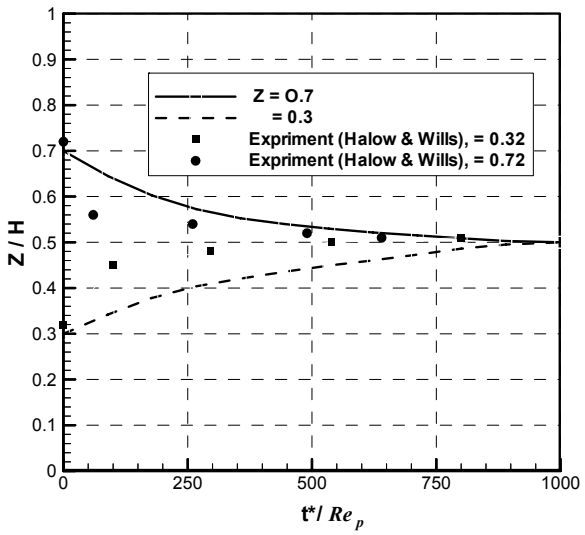

Fig. 5. Drop trajectories predicted in our simulation compared to those observed by Halow and Wills (1970) in a cylinderical Couette device. In the computation, Re_p = 0.225. In the expriment, Re_p =1.601, $\xi = 0.179$

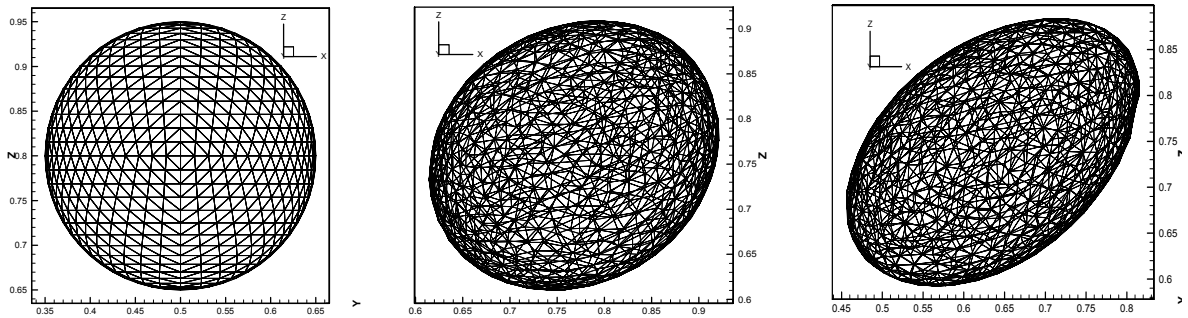

Fig. 6. Shape of a drop at (a) $t^* = 0$, (b) Re_b = 10, We = 0.09 , $t^* = 9$, (c) Re_b = 10, We = 0.27 , $t^* = 9$

Figure 8 shows the lateral migration of a drop at constant Re_b = 10 at two different values of Weber numbers: We = 0.0675 and We = 0.135. The x-velocity increases with increasing surface tension and the required time for drop migration to the centreline decreases.

Our simulations show that after an initial transient, the drop leads the local ambient fluid velocity for all runs. Initially, drop has a greater velocity than the undisturbed velocity. Figure 9 shows the slip velocity is normalized by the wall velocity U at Re_b = 5, 10, and 15 and We = 0.0675. The slip velocity is the difference between the drop velocity and the ambient fluid velocity at the centre of the drop for the undisturbed flow. The slip velocity plots agree qualitatively with the simulations of Halow and Willis, and

Feng *et al.* Hallow and Willis calculated the slip velocity by the Lorentz reflection method which is applicable only to Stokes flows. Curves presented by Feng *et al.* have small wiggles that result from the numerical method. They reported that the difference between their results is a measure of the inaccuracy of the simulation method. Curves plotted in Fig. 9 show similar results for the three values of Re_b.

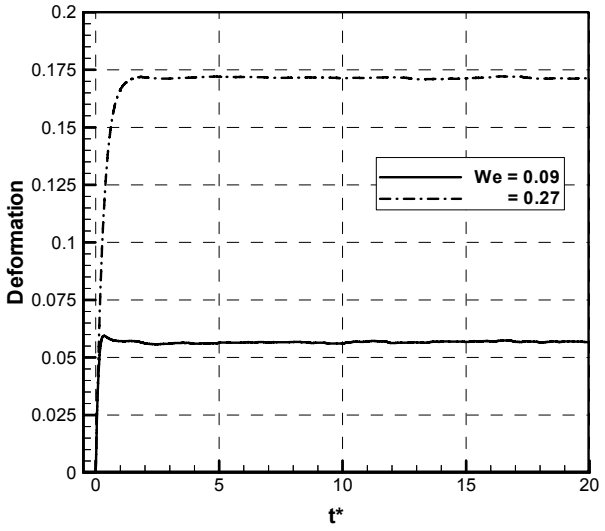

Fig. 7. Drop deformation at $Re_b = 10$

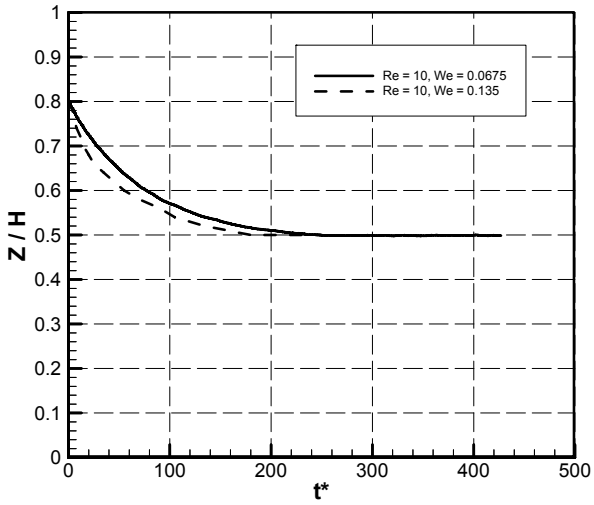

Fig. 8. Lateral migration of a drop in a simple shear flow at $Re_b = 10$, $We = 0.0675$ and $We = 0.135$

Based on these theories, the particle rotates with the local angular velocity of the flow field to within a small correction. This is a well-known result in Stokes flow (Feng *et al.*). Although experiments, theories and direct numerical simulations are in general agreement, the physical mechanisms of the lateral migration are unknown. We know three factors are possibly the cause of migration: 1. The wall repulsion (lubrication effect): Wall repulsion forces a drop away from a nearby wall to the centre of the channel (Feng *et al.*). 2. Perturbation effects: If the slip velocity leads the fluid, a drop will move into the slower stream and if the drop lags the fluid, the drop will move into the faster flow. The counterclockwise rotation of a drop may produce a lift force from both walls to the centre of the channel (Magnus type of

lift). Yang *et al*. reported that the slip angular velocity is the circulation for the free particle and it is shown to change its sign with the lift. 3. Force due to the deformation of the drop.

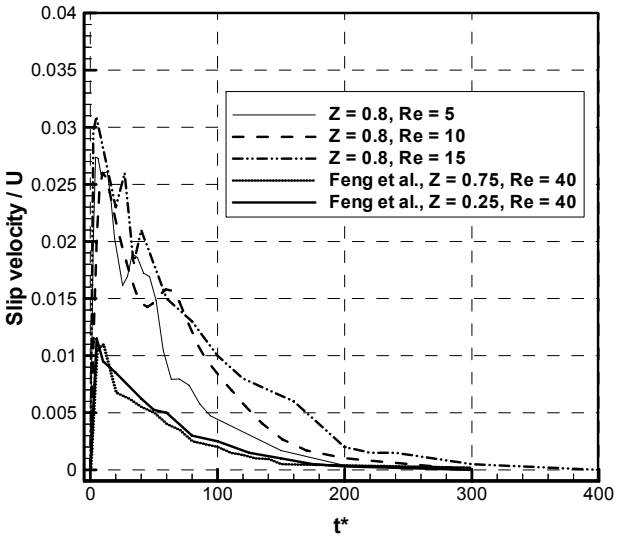

Fig. 9. Velocity of drops migrating in a simple shear flow at We = 0.0675
(Dimensionless time of Feng *et al.* results = t*/5)

Figure 10 and 11 show the x- and z-velocities of the centre of the drop normalized by the wall velocity U at Re_b = 5, 10, and 15 and We = 0.0675. When the x-velocity reaches the local undisturbed velocity, the slip velocity tends to zero. Curves plotted in these figures show that as time progresses, x-velocity decreases and z-velocity increases. In other words, the drop moves toward the centreline.

In Fig. 12, we plotted the curves of the lateral migration of a drop at Re_b = 5, 10, and 15 and We = 0.0675. Based on the curves of Figs. 10 and 11, it is predicted that the required time for the drop to reach equilibrium position increases as the Reynolds number increases at a fixed Weber number. This can be seen in Fig. 12.

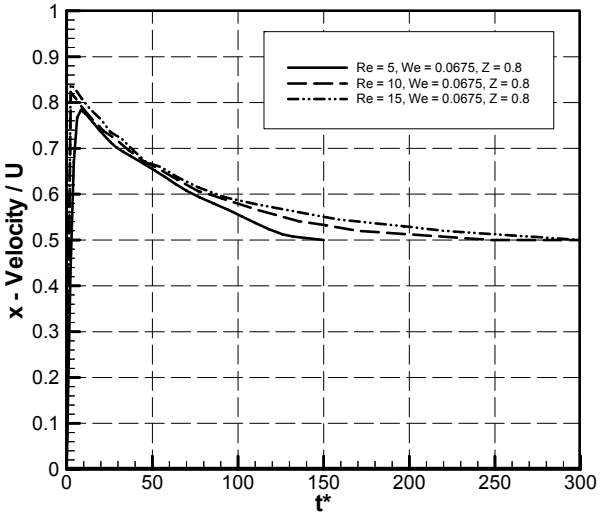

Fig. 10. x- velocity of drops migrating in a simple shear flow at We = 0.0675

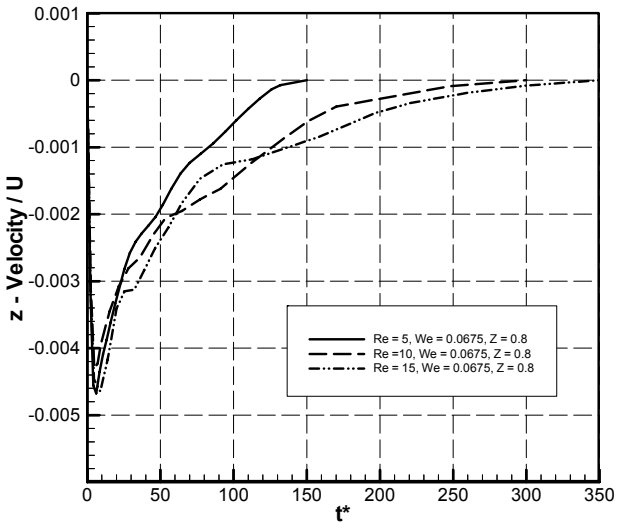

Fig. 11. z-velocity of drops migrating in a simple shear flow at We = 0.0675

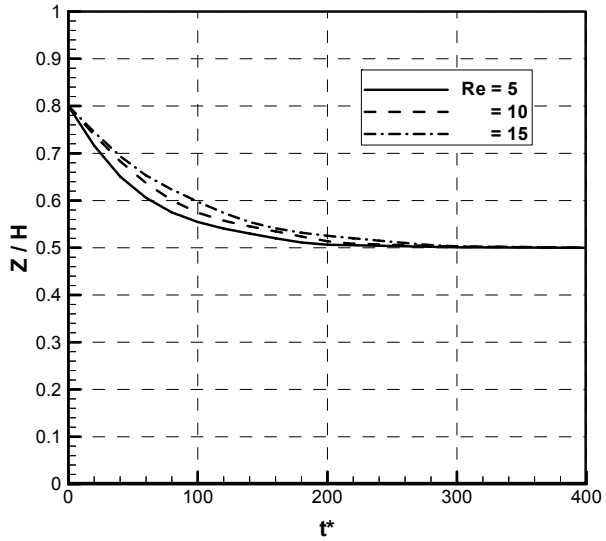

Fig. 12. Lateral migration of a drop in a simple shear flow at We = 0.0675

4. CONCLUSION

We have presented three-dimensional numerical simulations of the lateral migration of a single drop in a simple shear flow in a periodic domain. The full Navier-Stokes are solved by a finite difference/front tracking method. Most of the simulations for the lateral migration of deformable drops in a channel were restricted to the two-dimensional Stokes and potential flows. In this paper, we studied the migration of a drop in simple shear flow at finite Reynolds numbers by adding the advection terms to the governing equations

For the lateral migration of a drop in a Couette flow, the centreline of the channel is a stable equilibrium position. The deformation of a drop is an increasing function of the Weber number and the drop migrates faster to the centreline at higher Weber numbers. The x-velocity due to shear force increases with increasing surface tension and the required time for drop migration to the centreline decreases. Our simulations show that, after an initial transient, the drop leads the local ambient fluid velocity for all cases.

As time progresses, x-velocity decreases and z-velocity increases. When the x-velocity reaches the local undisturbed velocity, the slip velocity tends to zero, except during a short initial transient..

Our simulations agree qualitatively with simulations of Halow and Willis, Feng *et al.* and Yang *et al.*

REFERENCES

1. Taylor, G. I. (1934). The deformation of emulsions in definable fields of flow. *Proc, Ray. Soc*. (London) Vol. A146, PP.501-523.
2. Karnis, A. & Mason, S. G. (1967). Particle motions in shear suspension. Part 23. Wall migration of fluid drops. *I.Colloid Int. Sci*., Vol 24, pp. 164-169.
3. Halow, J. S. & Willis, G. B. (1970). Radial migration of spherical particles in Couette system. *AICHE J.*, Vol. 16, pp. 281-286.
4. Rallison, J. M. (1984). The deformation of small viscous drops and bubbles in shear flows. *Annu, Rev. Fluid Mech*., Vol. 16, pp. 45-66.
5. Mola, D., Hatamipour, M. S. & Moshfeghian, M. (1991). A simple model for prediction of pressure drop in horizontal two phase flows. *Iranian Journal of Science and Technology, Transaction B: Engineering*, Vol. 15, No. 2, pp. 177-185.
6. Magna, M. & Stone, H. A. (1993). Buoyancy-driven interactions between two deformable viscous drops. *J. Fluid Mech*, Vol. 256, pp. 647-683.
7. Zhou, H. & Pozrikidis, C. (1993). The flow of suspensions in channels: single files of drops. *Phys. Fluids*, Vol. A5, No. 2, pp. 311-324.
8. Feng, J., Hu, H. H. & Joseph, D. D. (1994). Direct simulation of initial value problems for the motion of solid bodies in a Newtonian fluid. Part2. Couette and Poiseuille flows. *J. Fluid Mech*, Vol. 277, pp. 271-301.
9. Li, X., Zhou, H. & Pozrikidis, C. (1995). A numerical study of the shearing motion of emulsions and foams. *J. Fluid Mech*, Vol. 286, pp. 374-404.
10. Loewenberg, M. & Hinch, E. (1996). Numerical simulation of a concentrated emulsion in shear flow. *J. Fluid Mech*., Vol. 321, pp. 395-419.
11. Esmaeeli, A. & Tryggvason, G. (1998). Direct numerical simulations of bubbly flows Part1. Low Reynolds number arrays. *J. Fluid Mech*, Vol. 377, pp. 313-345.
12. Mortazavi, S. S. & Tryggvasson, G. (1999). A numerical study of the motion of drop in poiseuille flow, part1: lateral migration of one drop. *J. Fluid Mech*, Vol. 411, pp. 325-350.
13. Esmaeeli, A. & Tryggvason, G. (1999). Direct numerical simulations of bubbly flows Part 2. Low Reynolds number arrays. *J. Fluid Mech*, Vol. 385, pp. 325-358.
14. Balabel, A., Binninger, B., Herrmann, M. & Peters, N. (2002). Calculation of droplet deformation by surface tension effects using the Level Set method. *J. Combustion Science and Technology*, Vol. 174 pp. 257-278.
15. Crowdy, D. G. (2003). Compressible bubbles in stokes flow. *J. Fluid Mech*., Vol. 476, pp. 345-356.
16. Yoon, Y., Borrell, M., Park, C. C. & Leal, G. (2005). Viscosity ratio effects on the coalescence of two equal-sized drops in a two-dimensional linear flow. *J. Fluid Mech*., Vol. 525, pp. 355-379.
17. Norman, J. T., Nayak, H. V. & Bonnecaze, T. B. (2005). Migration of buoyant particles in low-Reynolds-number pressure-driven flows. *J. Fluid Mech*., Vol. 523, pp. 1-35.
18. Yang, B. H., Wang, J., Hu, H. H., Pan, T. W. & Glowinski, R. (2005). Migration of a sphere in tube flow. *J. Fluid Mech*., Vol. 540, pp. 109-131.
19. Sibillo, V., Pasquariello, G., Simeone, M., Cristini, V. & Guido, S. (2007). Drop deformation in micro confined shear flow. *Phys. Rev. Lett.*, Vol. 97, pp. 2-4.

20. Zhao, X. (2007). Drop break up in dilute Newtonian emulsions in simple shear flow: new drop break up mechanism. *J. Rheology*, 51, pp. 367-192.
21. Unverdi, S. O. & Tryggvason, G.(1992). Comutaions of multi-fluid flows. *Phsics*, Vol. D60, pp. 70-83.
22. Ho, B. P. & Leal, L. G. (1974). Inertial migration of rigid spheres in two-dimensional unidirectional flows, *J. Fluid Mech*., Vol. 65, pp. 365-383.